

Fluorescence acquisition during hybridization phase in quantitative real-time PCR improves specificity and signal-to-noise ratio

Mohit Mehndiratta, Jayanth Kumar Palanichamy, Pradeep Ramalingam, Arnab Pal, Prerna Das, Subrata Sinha, and Parthaprasad Chattopadhyay
Department of Biochemistry, All India Institute of Medical Sciences, New Delhi, India

BioTechniques 45:625-634 (December 2008)
doi 10.2144/000112994

Quantitative real-time PCR (qPCR) is a standard method used for quantification of specific gene expression. This utilizes either dsDNA binding dyes or probe based chemistry. While dsDNA binding dyes have the advantage of low cost and flexibility, fluorescence due to primer dimers also interferes with the fluorescence of the specific product. Sometimes it is difficult, if not impossible, to standardize conditions and redesign primers in such a way that only specific fluorescence of the products of test and reference genes are acquired. Normally, the fluorescence acquisition in qPCR using dsDNA binding dyes is done during the melting phase of the PCR at a temperature between the melting points of primer dimers and the specific product. We have modified the protocol to acquire fluorescence during the hybridization phase. This significantly increased the signal-to-noise ratio and enabled the use of dsDNA binding dyes for mRNA quantification in situations where it was not possible when measurement was done in the melting phase. We have demonstrated it for three mRNAs, E6, E7, and DNMT1 with β -actin as the reference gene, and for two miRNAs. This modification broadens the scope of qPCR using dsDNA binding dyes.

INTRODUCTION

The techniques available to study mRNA expression are Northern blotting, quantitative real-time PCR, and microarrays. While Northern blotting is cumbersome, microarrays are used for high-throughput but less-sensitive analysis. Thus qPCR remains the gold standard for comparing gene expression levels (1–3). qPCR is done either using probe-based chemistry or dye-based chemistry. Though more specific, the main drawback of probes is the requirement of expensive gene-specific probes. Dye-based chemistry is comparatively economical as it requires only gene-specific primers and is generally the routine method. The dyes used include SYBR green, Syto 9, and EvaGreen which bind only to dsDNA. The main drawback of dye-based quantification is non-specific amplification or the formation of primer dimers, which also contribute to the increase in fluorescence and can thus decrease the signal-to-noise-ratio (SNR) where the

fluorescence of the specific product is taken as the signal and the fluorescence of the primer dimer is taken as the noise.

Quantification of product is usually done by measuring fluorescence at a temperature above the melting temperature (T_m) of the nonspecific product, but below the T_m of the specific product (4). This can be defined as acquisition in the melting phase, since the temperature is increased above the extension temperature (usually 72°C) to a point where the primer dimers have melted but the specific product has not yet melted. However, primer dimer kinetics are seldom predictable, and on many occasions longer nonspecific products are formed with a T_m close to or almost overlapping that of the product, which interferes with the exact quantitation of the product alone. This cannot always be avoided by reducing the primer concentration, and sometimes constraints of template sequence preclude alternate primer design. This is especially true for quantitation of miRNAs. When gene expression

studies are done using an internal reference gene, it is always better to choose a temperature for fluorescence measurement that avoids overlaps in the melting profile of the specific product and primer dimers of both target and reference genes, since it enables the amplification of both genes in one PCR run (5–8). Though not absolutely essential, it helps in avoiding run-to-run variations and repeated freeze-thaw cycles, and also saves on time. All these limit the use of dye-based chemistry in gene expression studies.

Instead of acquiring fluorescence in the melting phase, we have acquired fluorescence in the hybridization phase by including a step to denature the specific product and primer dimers and then decrease the temperature to a point where the specific product has hybridized but the primer dimers have not. We have investigated whether acquisition during the hybridization phase would improve the discrimination between the primer dimers and the specific products, and the SNR of the measurement. This was done for three mRNAs: human papilloma virus (HPV) genes E6 and E7, eukaryotic gene DNMT1, and small RNAs miR27 and U6 snRNA.

MATERIALS AND METHODS

U87MG, SiHa, and MCF-7 cell lines (ATCC, Manassas, VA, USA) were used for experiments and were maintained in DMEM (Sigma-Aldrich, St. Louis, MO, USA) supplemented with 10% FCS (Sigma-Aldrich), 3.7 g/dL sodium bicarbonate, ciprofloxacin (10 μ g/mL), and 5% CO₂ at 37°C. RNA was extracted using TRIzol reagent (Invitrogen, Carlsbad, CA, USA) as per the manufacturer's protocol. miRNAs were isolated using the Purelink miRNA isolation kit (Invitrogen). After DNase (Ambion, Austin, Texas, USA) treatment, RNA was quantified using a spectrophotometer (Nano Drop ND-1000; Thermo Fisher Scientific, Waltham, MA, USA). cDNA synthesis was done using 1 μ g of RNA, RETROscript reverse transcriptase (RT) (Ambion), and random decamers. For miRNAs, cDNA synthesis was done using stem-loop primers (9).

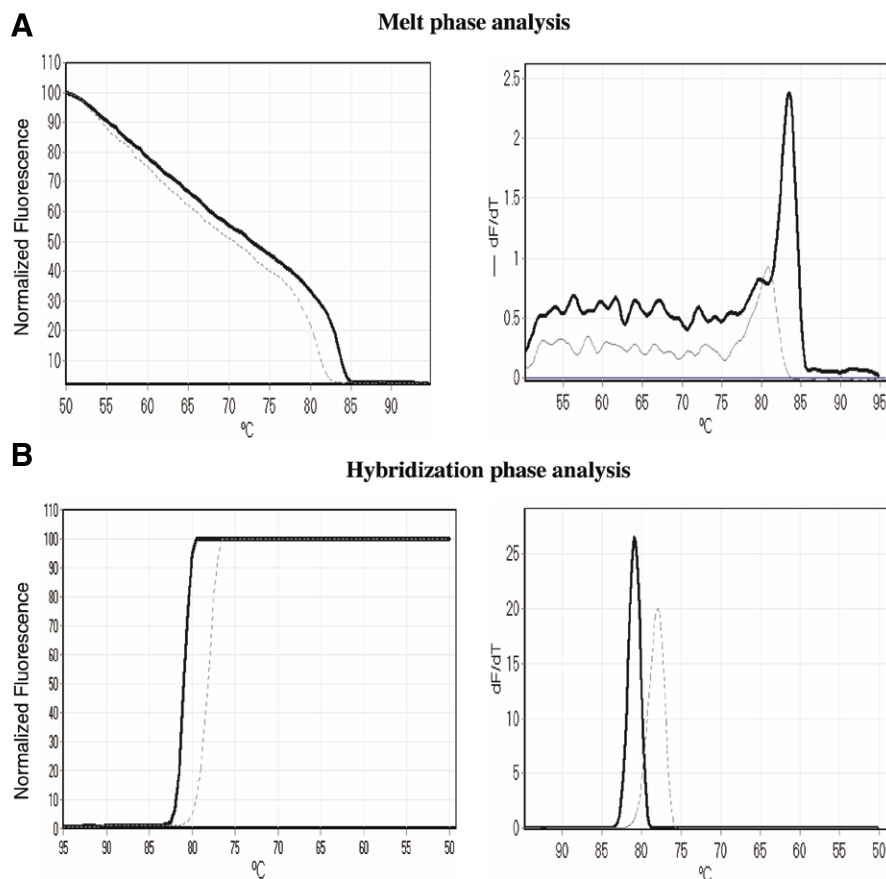


Figure 1. The (A) melt and (B) hybridization curves and their analyses of E6 specific product (solid line) and its primer dimer (broken line). dF/dT refers to the rate of change of fluorescence with increase or decrease in temperature. Improved SNR and PSS in the hybridization curve at 80°C (18.90 and 89.90, respectively) compared with that in the melt curve at 80°C (1.52 and 11.31, respectively) is observed. Obvious interference between E6 specific product and E6 primer dimers in the melt curve is significantly less in the hybridization curve.

Real-Time PCR

Quantitative PCR reactions and threshold value (C_t) calculations were done on a Rotor-Gene 6000 (Corbett Research, Mortlake, Australia) using the software provided. Amplification efficiencies of individual reactions were calculated using the Rotor-Gene 6000 (Corbett Research) software.

PCR reactions were carried in 10 μ L reaction volumes: 2.5 μ L of 1:5 diluted cDNA, 0.5 μ L of primer mix (0.5 pmol/ μ L as final concentration of each primer), 1 μ L of 10 \times *Taq* Buffer A, 0.5 U *Taq* DNA polymerase (both from Bangalore Genei, Bangalore, India), 1 μ L Syto 9 (Invitrogen, Carlsbad, CA, USA), 0.25 μ L of 10 mM dNTPs (Fermentas Inc, USA), and 4.6 μ L of nuclease-free water (Ambion). In case

of reactions involving standard curves, cDNA dilutions (x , $x/2$, $x/4$, and $x/8$) were prepared in nuclease-free water. All the samples were put up in triplicates. The real-time PCR products were run on an agarose gel to rule out any cDNA contamination in the no-template control (NTC) sample.

The qPCR cycling conditions for melt phase SYTO 9 fluorescence acquisition were 40 cycles of 95°C for 10 s, 55–60°C (depending on T_m of primers) for 20 s, 72°C for 30 s, and 78–85°C [fluorescence acquisition was determined by previous high-resolution melt (HRM) analysis] for 5 s. The qPCR cycling conditions for hybridization phase SYTO 9 fluorescence acquisition were 40 cycles of 95°C for 5 s, 79–82°C [fluorescence acquisition was

determined by previous high-resolution hybridization (HRH) analysis] for 5 s, 95°C again for 10 s, 55–60°C (depending on T_m of primers) for 20 s, and 72°C for 30 s. Then, HRM and HRH were undertaken by measuring SYTO 9 fluorescence at 0.5°C/s intervals while ramping 50–95°C and 95–50°C, respectively.

Signal-to-Noise Ratio (SNR) and Product-Specific Signal (PSS) Calculation

Normalized fluorescence units (NFU) were used to calculate the SNR and PSS. Normalization allows all the curves to be compared with the same starting and ending fluorescent signal level to aid interpretation and analysis. Using the Rotor-Gene 6000 (Corbett Research) software, two regions each are identified in the hybridization curve (pre- and post-hybridization phase) and melting curve (pre- and post-melting phase) in the pre-hybridization and post-melt phase, respectively. The fluorescence of pre-hybridization and post-melt phases is taken as 0, while that of post-hybridization and pre-melt phases is taken as 100. All the values within these two regions are adjusted to a value within this 0–100 range.

SNR at a particular temperature was calculated as the ratio of NFU in the tube containing cDNA and reaction mixture to the NFU in the no-template control tube.

PSS was calculated by subtracting the NFU in the tube containing no-template control from NFU in the tube containing cDNA.

The NFU levels were measured for the same temperature and SNR were calculated separately using both the high-resolution melt or hybridization graphs (Table 1).

Calculation of SNR and PSS using these equations might lead to a slight underestimation of the real SNR and PSS due to competition during amplification between the specific template and primer dimers (10). However, the calculation of amplification efficiency, threshold cycle value, and quantification are not affected, as SNR and PSS are used only to find the temperature at which fluorescence is measured.

Short Technical Reports

Table 1. SNR and PSS Comparison

Temp (°C)	Melt Phase Analysis				Hybridization Phase Analysis			
	Actin SNR	Actin PSS	DNMT1 SNR	DNMT1 PSS	Actin SNR	Actin PSS	DNMT1 SNR	DNMT1 PSS
78	1.45	12.59	12.91	36.91	1.68	40.54	112.16	99.11
79	1.54	13.61	12.81	34.63	2.97	66.37	126.07	99.21
80	1.68	14.92	11.18	31.80	6.49	84.59	139.41	99.28
81	1.93	16.84	9.30	28.86	16.60	93.97	145.90	99.31
82	2.39	19.12	10.23	27.03	48.52	97.94	133.43	82.41
83	3.23	21.29	8.03	23.58	110.92	99.10	41.68	24.97
84	4.63	22.54	7.64	18.08	142.64	99.30	3.23	1.35
85	6.75	22.70	5.46	11.01	116.16	78.36	1.29	0.18
	Actin SNR	Actin PSS	E6 SNR	E6 PSS	Actin SNR	Actin PSS	E6 SNR	E6 PSS
78	1.36	11.34	1.21	6.68	2.15	53.50	1.76	43.20
79	1.42	12.09	1.31	8.62	3.28	69.48	4.75	78.93
80	1.49	13.02	1.52	11.31	5.68	82.40	18.90	89.90
81	1.65	14.82	2.29	16.82	12.26	91.85	31.89	45.22
82	1.88	16.71	4.90	20.83	33.83	97.04	6.37	5.37
83	2.30	19.02	6.97	16.36	69.11	98.55	1.37	0.34
84	4.02	23.72	3.28	5.74	83.44	98.80	1.19	0.18
85	9.18	26.18	1.09	0.23	97.18	98.97	1.25	0.22
	Actin SNR	Actin PSS	E7 SNR	E7 PSS	Actin SNR	Actin PSS	E7 SNR	E7 PSS
78	1.54	14.75	2.16	20.10	4.26	76.53	34.53	97.10
79	1.70	16.52	3.23	24.53	8.34	88.01	45.96	85.36
80	1.98	18.75	5.81	27.51	18.53	94.60	34.85	52.25
81	2.40	20.94	7.62	26.57	48.81	97.95	17.29	22.72
82	3.26	23.25	8.56	24.55	96.08	98.96	4.62	5.57
83	4.74	24.38	8.51	21.66	126.85	99.21	1.19	0.28
84	6.51	24.10	6.02	15.66	152.99	85.20	0.99	-0.01
85	8.34	23.19	2.62	4.54	71.33	48.83	1.03	0.03
	U6 SNR	U6 PSS	miR27 SNR	miR27 PSS	U6 SNR	U6 PSS	miR27 SNR	miR27 PSS
78	1.43	8.69	2.44	17.38	6.15	83.75	42.59	97.65
79	1.67	10.85	3.36	19.17	11.10	90.99	58.79	98.30
80	1.95	12.12	4.39	19.27	22.00	87.95	64.53	88.07
81	2.15	11.87	5.51	18.72	23.05	41.19	40.79	53.27
82	2.19	9.77	5.58	16.24	6.13	5.84	17.60	19.87
83	2.10	6.53	5.00	12.46	1.67	0.53	5.11	4.05
84	1.78	3.32	3.69	7.78	1.11	0.10	1.93	0.78
85	1.23	0.74	2.21	3.48	1.00	0.00	1.25	0.20

Comparison of SNR and PSS of fluorescent signals acquired during the melt and hybridization phase analyses. Shaded regions represent high SNR and PSS values.

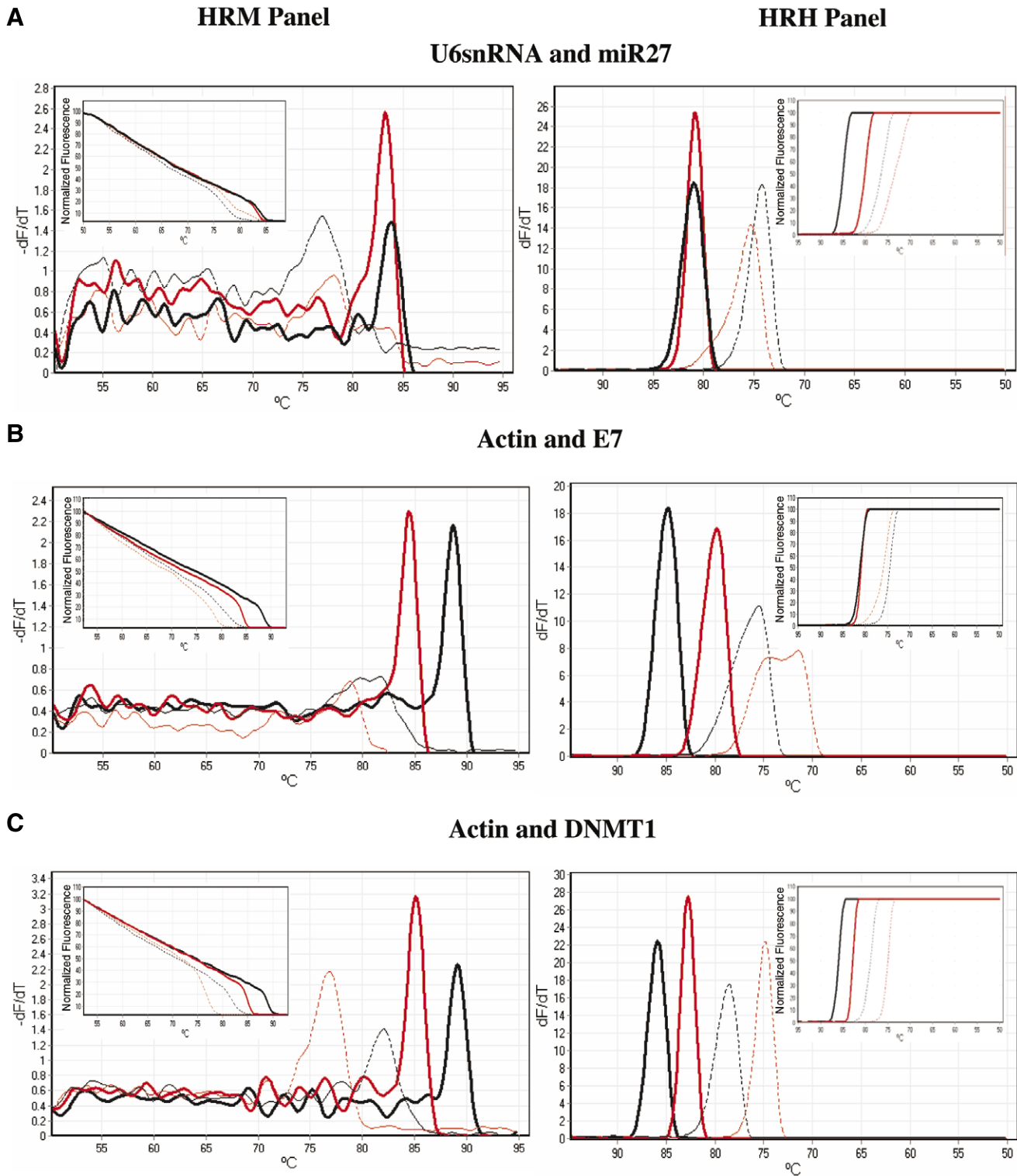


Figure 2. Comparison of the melt and hybridization curve analyses of (A) U6snRNA, (B) E7, and (C) DNMT1 (solid red lines) and their reference genes miR27 and actin (solid black lines) along with their respective no template controls (broken lines of corresponding color). Insets show the normalized melt and hybridization curves. (A) U6 and miR27: In the melt phase the primer dimers overlap significantly with the specific product whereas in the hybridization curve they are better discriminated. (B) Actin and E7: Primer dimers of β -actin melt overlap with the E7-specific product in the melt phase. In the hybridization phase, the distinction between the actin primer dimers and the E7-specific product is enhanced. (C) Actin and DNMT1: A similar situation is observed here where β -actin primer dimers interfere with the DNMT1-specific product in the melt phase, but a clear demarcation between them is observed in the hybridization phase.

Statistical Analysis

Relative error between dilutions was calculated using the equation

$$\text{Rel. error} = \frac{E^{\Delta Ct} - CDD}{CDD},$$

[Eq. 1]

where E is the amplification efficiency, ΔCt is the difference in Ct values (i.e., Ct value of undiluted sample – Ct value of diluted sample), and CDD is the cDNA dilution.

P values were calculated using the paired t -test. The sequences of primers used are given in Supplementary Table 1 (available online at www.BioTechniques.com).

RESULTS AND DISCUSSION

The melting and hybridization profile of the PCR products for the genes studied are shown in Figures 1 and 2, and the calculated SNR and PSS are shown in Table 1.

During real-time PCR, when fluorescence is measured around the temperature that gives a higher SNR, it gives a better approximation of the product formed at each cycle, since at that temperature, most of the smaller and heterogeneous primer dimers are single-stranded and non-fluorescent, while larger specific-product molecules are double-stranded and, hence, fluorescent. At the same temperature, endpoint PSS in the melting or hybridization profiles should also be acceptably high so that there is an adequate product-specific rise in fluorescence above the threshold. The shaded regions in Table 1 denote those ranges that meet the above criteria.

Real-time PCR of E6, using primers designed by the Primer3 online program (primer3.sourceforge.net) illustrates these points. (Figure 1) When analyzed by an HRM profile, primer dimers and product melted between 77–82°C and 81–85°C, respectively, whereas in HRH analysis, hybridization of primer dimers and product occurred between 76–81°C and 79–82°C, respectively.

If real-time PCR is carried out with fluorescence detection in the melting phase at a temperature decided on the basis of the HRM profile (82°C), PSS is too low to show up above the threshold during real-time PCR even though the SNR is high. However, carrying out real-time PCR with fluorescence detection in the hybridization phase at a temperature determined from the HRH curve (80°C) resulted in a high PSS with an acceptable SNR ratio and a successful quantitation. This result was repeatable in quantitation of E7, DNMT1, and miR27 (Table 1).

Choosing the optimum temperature at which to measure fluorescence during each cycle of real-time PCR becomes more difficult in certain situations when the decision is based on HRM analysis (Figure 2, HRM panel). In many cases, there is a significant overlap in the temperature range of high SNR and PSS (Table 1) between the reference gene (β -actin for mRNA, U6 snRNA for small RNA) and target gene (E6, E7, DNMT1) and miR27, thus providing us with no single temperature option where the fluorescence of both the target and reference gene during real-time PCR can be acquired with high SNR and PSS values. However, in such cases, the optimum temperature for fluorescence detection can easily be identified from HRH curves (Figure 2), as well as the SNR and PSS values of the reference and the target genes (Table 1). Moreover, PSS values at different temperatures are in general higher during hybridization phase than when measured during melting phase (Table 1).

It has to be remembered that while DNA denaturation (local melting followed by unzipping) follows first-order kinetics, DNA renaturation takes place in two phases: the contact-forming phase that follows second-order kinetics, and the zipping phase that follows first-order kinetics (11). This may explain the difference in the melting and hybridization profile of PCR products as observed.

Fluorescence acquisition in the hybridization phase also led to a significant improvement ($P < 0.05$) in the amplification efficiencies of four out of five genes tested (Supplementary

Materials, Table 2, available online at www.BioTechniques.com), while the detection limit remained the same whether fluorescence was acquired in the melt or in the hybridization phase (data not shown).

To further confirm the accuracy of qPCR with fluorescence acquisition in the hybridization phase, standard curves were obtained with double dilution of cDNA for the E6 gene and U6 snRNA. The R^2 for E6 mRNA was 0.961 when measured during the melt phase qPCR (80°) and 0.998 during the hybridization phase (80°). The relative error between dilutions in the hybridization phase was 0.19 which is significantly lower ($P = 0.03$) than that in the melting phase, which was 0.40 (Supplementary Materials, Figure 1, available at www.BioTechniques.com). Similarly, the R^2 value for U6 snRNA in the melt phase was 0.978 and 0.994 in the hybridization phase. The relative error was also significantly lower ($P = 0.002$) in the hybridization phase (0.16) than the melting phase (0.94). (Supplementary Materials, Figure 2, available online at www.BioTechniques.com).

These results demonstrate improved accuracy when quantification is done using fluorescence acquisition in the hybridization phase at a temperature optimized by HRH analysis.

Our results convincingly demonstrate that when there is interference due to primer dimers in real-time PCR, quantification done with fluorescence acquisition during the hybridization phase at a temperature determined by HRH analysis results in better discrimination between nonspecific fluorescence from primer dimers and product-specific fluorescence, as well as an increased SNR compared with fluorescence acquisition during melt phase. The same is true when comparing target gene expression with reference gene expression. It is possible that this is due to the difference in the kinetics of DNA denaturation and renaturation.

This modification in the phase of fluorescence acquisition in qPCR will be helpful when there is an overlap between the melt curves of fluorescence of nonspecific primer dimers and the specific product, and extend

Give your marketing programs a **LIFT!**



Reach over
125,000
Life Science
Professionals

Let Informa Life Sciences mailing lists spearhead your next campaign

If you are looking to maximize your marketing efforts to professionals who work in all aspects of pharma and biotech, you need a resource that gives you access to your best responders — and that's Informa Life Science mailing lists.

Cultivated from our targeted subscriber base of life science professionals, our lists give you **the best chance** of delivering your brand and offer to this market.

Let us locate the **right decision-makers** in your market segment:

- Over 125,000 life science professionals
- \$25 billion in purchasing power
- Segmentation including function, title and laboratory technique
- worldwide reach

Life science marketing lists with **more life**.
For more information, call **(212) 520-2729**

Informa Life Sciences **DATA**
Target prospects with responsive lists

the scope of qPCR using dsDNA binding dyes resulting in increased flexibility and reduced costs.

ACKNOWLEDGEMENTS

We would like to thank Mathura Prasad and Satish Kumar for their technical support. We would like to acknowledge the Council of Scientific and Industrial Research (sanction no. 27/138/05/EMRII), the Department of Biotechnology, Government of India (sanction no. BT/01/COE/05/13), and the Indian Council of Medical Research (sanction no. 63/12/2002-BMS) for their financial assistance.

COMPETING INTERESTS STATEMENT

The authors declare no competing interests.

REFERENCES

1. Roth, C.M. 2002. Quantifying gene expression. *Curr. Issues Mol. Biol.* 4:93-100.
2. Pfaffl, M.W. 2001. A new mathematical model for relative quantification in real-time RT-PCR. *Nucleic Acids Res.* 29:e45.
3. Freeman, W.M., S.J. Walker, and K.E. Vrana. 1999. Quantitative RT-PCR: pitfalls and potential. *BioTechniques* 26:112-125.
4. Ball, T.B., F.A. Plummer, and K.T. Hay-Glass. 2003. Improved mRNA quantitation in LightCycler RT-PCR. *Int. Arch. Allergy Immunol.* 130:82-86.
5. Rutledge, R.G. and C. Cote. 2003. Mathematics of quantitative kinetic PCR and the application of standard curves. *Nucleic Acids Res.* 31:e93.
6. Ramakers, C., J.M. Ruijter, R.H. Deprez, and A.F. Moorman. 2003. Assumption-free analysis of quantitative real-time polymerase chain reaction (PCR) data. *Neurosci. Lett.* 339:62-66.
7. Goidin, D., A. Mamessier, M.J. Staquet, D. Schmitt, and O. Berthier-Vergnes. 2001. Ribosomal 18S RNA prevails over glyceraldehyde-3-phosphate dehydrogenase and beta-actin genes as internal standard for quantitative comparison of mRNA levels in invasive and noninvasive human melanoma cell subpopulations. *Anal. Biochem.* 295:17-21.
8. Schmittgen, T.D. and B.A. Zakrajsek. 2000. Effect of experimental treatment on housekeeping gene expression: validation by real-time, quantitative RT-PCR. *J. Biochem. Biophys. Methods* 46:69-81.
9. Chen, C., D.A. Ridzon, A.J. Broomer, Z. Zhou, D.H. Lee, J.T. Nguyen, M. Barbisin, N.L. Xu, et al. 2005. Real-time quantification of microRNAs by stem-loop RT-PCR. *Nucleic Acids Res.* 33:e179.
10. Alvarez, M.J., A.M. Depino, O.L. Podhajcer, and F.J. Pitossi. 2000. Bias in estimations of DNA content by competitive polymerase chain reaction. *Anal. Biochem.* 287:87-94.
11. Murugan, R. 2003. A stochastic model on DNA renaturation kinetics. *Biophys. Chem.* 104:535-541.

Received 7 June 2008; accepted 18 September 2008.

Address correspondence to Parthaprasad Chattopadhyay, Room no. 3037, Department of Biochemistry, All India Institute of Medical Sciences, New Delhi, India 110029. email: parthoaiims@hotmail.com

To purchase reprints of this article, contact: Reprints@BioTechniques.com